Eur. Phys. J. D **39**, 445–451 (2006)
DOI: 10.1140/epjd/e2006-00127-x

THE EUROPEAN PHYSICAL JOURNAL D

Threshold behavior of semi-linear photorefractive oscillator

P. Mathey[1,a], M. Grapinet[1], H.R. Jauslin[1], B. Sturman[2], D. Rytz[3], and S. Odoulov[4]

[1] Laboratoire de Physique de l'Université de Bourgogne, UMR CNRS 5027, 9 avenue A. Savary, B.P. 47870, 21078 Dijon, France
[2] Institute of Automation and Electrometry, Russian Academy of Sciences, 630090 Novosibirsk, Russia
[3] Forschunginstitute für mineralische and metallische Werkstoffe, Edelsteine/Edelmetalle GmbH, Struhtstrasse 2, Wackenmühle, 55743 Idar-Oberstein, Germany
[4] Institute of Physics, National Academy of Sciences, 252650 Kiev, Ukraine

Received 23 November 2005 / Received in final form 14 March 2006
Published online 13 June 2006 –

Abstract. A general analysis of the threshold behavior for the photorefractive semi-linear oscillator is performed within the linear approximation on the basis of the classical wave-coupling model. This analysis shows that the well known particular results on the frequency degenerate oscillation are valid only within a restricted range of the external parameters. The theory specifies the conditions for onset and properties of the frequency non-degenerate oscillations, including the necessary values of the coupling strength, pump intensity ratio, the increments of the instability, and the frequency splits. Important generalizations of the basic model are considered.

PACS. 42.65.Hw Phase conjugation; photorefractive and Kerr effects – 05.45.-a Nonlinear dynamics and chaos – 42.65.Pc Optical bistability, multistability, and switching, including local field effects – 42.65.Sf Dynamics of nonlinear optical systems; optical instabilities, optical chaos and complexity, and optical spatio-temporal dynamics

1 Introduction

Strong photorefractive nonlinearity inherent in many electro-optic materials (including ferroelectrics and semiconductors) has led to the emergence of numerous new optical schemes and devices employing the advantages of the phase conjugation and optical oscillation [1–5]. A generic feature of such schemes is a complete (or almost complete) frequency degeneracy. A variety of output characteristics is achieved due to a wide range of possibilities for optical feedbacks between the oscillation and pump waves.

The semi-linear photorefractive oscillator was one the first nonlinear devices of this type [6]. Its cavity is formed by an ordinary feedback mirror and a photorefractive crystal that serves as an amplifying phase-conjugate mirror pumped by two counter-propagating coherent light waves of the same frequency, see Figure 1a. Owing to its apparent simplicity, this scheme serves often as a sample for the investigation of dynamic properties of photorefractive oscillators, bifurcations including the threshold behavior and the transition to chaos [7–10].

The operation of the semi-linear oscillator is based on the buildup of refractive index gratings (by different pairs of pump and oscillation waves) and diffraction from these gratings. By playing with the coherence length and/or material properties, one can realize the distinct cases of transmission and reflection gratings. The basic dynamic equations for these cases are well-known [2]. For the most common gradient (diffusion) photorefractive response and frequency degenerate oscillation, these nonlinear equations admit exact steady-state solutions incorporating the effect of pump depletion [3,11]. In the transmission case, these solutions correspond to the soft and hard excitation scenarios for different values of the pump ratio r and the feedback mirror reflectivity R. In the reflection case, the steady states correspond to the soft threshold behavior.

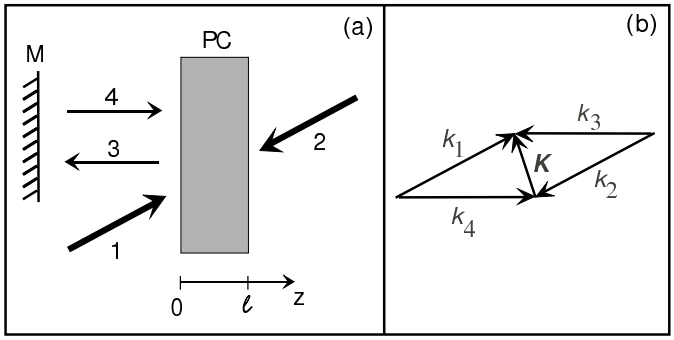

Fig. 1. (a) Schematic diagram of the semi-linear photorefractive oscillator; M is the ordinary feedback mirror, PC is the photorefractive crystal. (b) The corresponding wave-vector diagram.

[a] e-mail: pmathey@u-bourgogne.fr

Experiment shows [12,13] that changing the pump ratio can result in a frequency bifurcation of the oscillation mode for the transmission case and diffusion photorefractive response: the single-frequency oscillation transforms into a two-frequency oscillation. A first explanation of this transition was given on the basis of a heuristic treatment of the influence of the frequency splitting on the oscillation threshold [12–14]. The key point of this analysis is the assumption of an automatic fulfillment of phase matching for the oscillation wave during a round trip in the cavity.

In this paper we present the general theory of the threshold and near-threshold behavior of the semi-linear oscillator. It is based on the linearized conventional basic model with proper boundary conditions for the oscillation wave amplitudes. Our analysis incorporates uniformly the intensity and phase matching conditions for the oscillation. Our theory says first that the heuristic assumption of an automatic fulfillment of the phase matching is not compatible with the basic model; this leads to quantitative and qualitative changes of the predicted in [12–14] threshold behavior. Second, the theory shows that the assumption of a degenerate oscillation and the known exact steady-state solutions are valid only within a restricted range the control parameters. Our analysis specifies the conditions for the non-degenerate oscillations (the necessary values of the coupling strength, the pump intensity ratio, etc.) and the values of the frequency split. It shows, in particular, that there are regions of the experimental parameters where degenerate and non-degenerate oscillation modes exist separately and the regions where these modes compete with each other. Our theory fills thus an obvious gap in the knowledge of the operation regimes of the semi-linear oscillator. Possibilities for generalization of the basic model and explanation of available results are considered. The method of the temporal analysis which is used in this paper is to be new in the field of photorefractive oscillators; it can be applied to other oscillation schemes.

2 Basic relations

2.1 Coupled-wave equations

The wavevector diagram for the semi-linear photorefractive oscillator in question is presented in Figure 1b. We have two counter-propagating pump waves, 1 and 2, and two counter-propagating oscillation waves 3 and 4. Two wave pairs, $1,4$ and $3,2$, contribute to the recording of the transmission grating with the grating vector $\mathbf{K} = \mathbf{k}_1 - \mathbf{k}_4 = \mathbf{k}_3 - \mathbf{k}_2$. Pump waves 1 and 2 diffract from this grating to oscillation waves 4 and 3, respectively; the reverse diffraction processes are important for sufficiently strong oscillation waves.

The set of equations for this four-wave coupling scheme is standard [2,3]. It consists of diffraction equations for the complex amplitudes of the light waves $A_{1,2,3,4}$,

$$\frac{\partial A_1}{\partial z} = \nu^* A_4, \qquad \frac{\partial A_2}{\partial z} = \nu A_3,$$
$$\frac{\partial A_3}{\partial z} = -\nu^* A_2, \qquad \frac{\partial A_4}{\partial z} = -\nu A_1, \tag{1}$$

and a material equation for the grating amplitude ν,

$$t_r \frac{\partial \nu}{\partial t} + \nu = \frac{\gamma_0}{I_0}(A_1^* A_4 + A_2 A_3^*). \tag{2}$$

The asterisk stands for the complex conjugation, γ_0 is a coupling constant (it is real for the diffusion response), $I_0 = I_1 + I_2 + I_3 + I_4$ is the total intensity, $I_i = |A_i^2|$ ($i = 1,2,3,4$) is the intensity of the ith wave, and $t_r \propto 1/I_0$ is the photorefractive response time.

The boundary conditions for waves 1 to 4 read:

$$A_1(0,t) = A_1^0 = const, \quad A_2(l,t) = A_2^l = const,$$
$$A_3(l,t) = 0, \qquad A_4(0,t) = \sqrt{R}\, e^{i\phi_0}\, A_3(0,t), \tag{3}$$

where l is the crystal thickness, R is the reflection coefficient of the feedback mirror, and ϕ_0 is a constant phase shift determined by the distance to the mirror.

The following conservation laws are fulfilled:

$$I_1(z,t) + I_4(z,t) \equiv I_+(t),$$
$$I_2(z,t) + I_3(z,t) \equiv I_- = I_2^l = const. \tag{4}$$

According to these relations, the total intensity $I_0 = I_+ + I_-$ and the response time t_r are generally functions of t.

In addition to the mirror reflectivity R, the control parameters for this scheme are the pump ratio $r = I_2^l/I_1^0$ and the coupling strength $g = \gamma_0 l$.

2.2 Undepleted pump approximation

When the oscillation waves 3 and 4 are weak, $I_{3,4} \ll I_{1,2}$, one can neglect their influence on the pump and use the undepleted pump approximation. Within this approximation we have $A_1 = A_1^0 = const$, $A_2 = A_2^l = const$, $I_0 = I_1^0 + I_2^l = const$, and the variables A_3^*, A_4, and ν obey a closed set of linear differential equations,

$$\frac{\partial A_4}{\partial z} = -\nu\, A_1^0$$
$$\frac{\partial A_3^*}{\partial z} = -\nu\, A_2^{l*}$$
$$t_r \frac{\partial \nu}{\partial t} + \nu = \frac{\gamma_0}{I_0}\,(A_1^{0*} A_4 + A_2^l A_3^*), \tag{5}$$

with a constant response time t_r. Coupling of the amplitude A_4 with the complex conjugate amplitude A_3^* is the fingerprint of the phase conjugation in our optical scheme.

2.3 Steady-state solutions

Set (5) admits steady-state solutions of the form

$$\begin{aligned} A_3(z,t) &= A_3^+(z)\exp(+i\Omega t) \\ A_4(z,t) &= A_4^-(z)\exp(-i\Omega t) \\ \nu(z,t) &= \nu^-(z)\exp(-i\Omega t), \end{aligned} \tag{6}$$

where Ω is an arbitrary frequency detuning. The spatial amplitude ν^- is algebraically expressed through A_3^+ and A_4^-. The coordinate dependence of the wave amplitudes obeys a linear second-order set of differential equations which follows immediately from equations (5). The general solution for A_4^- and A_3^{+*} is given by

$$\begin{pmatrix} A_4^- \\ A_3^{+*} \end{pmatrix} = c_1 \begin{pmatrix} -A_2^l \\ A_1^{0*} \end{pmatrix} + c_2 \begin{pmatrix} A_1^0 \\ A_2^{l*} \end{pmatrix} e^{\Gamma_0 z}, \tag{7}$$

where c_1 and c_2 are arbitrary complex constants and the rate of spatial changes Γ_0 is

$$\Gamma_0 = -\frac{\gamma_0}{1 - i\Omega t_r}. \tag{8}$$

We are interested in a steady-state solution that meets the boundary condition $A_3^+(l) = 0$. This solution describes the steady-state transformation of the incident wave 4 (which is detuned by Ω with respect to the pump) into a counter-propagating wave 3 (which is detuned by $-\Omega$). Such a transformation is inherent in the phase-conjugation processes. It is easy to find from equations (7) that the amplitude ratio $\rho(\Omega) = A_3^{+*}(0)/A_4^-(0)$, characterizing the phase conjugation, is given by

$$\rho(\Omega) = \frac{A_1^{0*} A_2^{l*} \left(1 - e^{\Gamma_0 l}\right)}{I_1^0 + I_2^l\, e^{\Gamma_0 l}}. \tag{9}$$

The replacement $\Omega \to -\Omega$ transforms $A_{3,4}^{\pm}$ to $A_{3,4}^{\mp}$. Therefore we have $\rho(-\Omega) = A_3^{-*}(0)/A_4^+(0)$. As follows from equation (8), it is sufficient to replace Γ_0 by Γ_0^* in equation (9) to obtain $\rho(-\Omega)$. In the case $\Omega = 0$ we return to the known expression for the intensity ratio $|\rho|^2$ characterizing the phase conjugation [3], $|\rho|^2 = \sinh^2(g/2)/\cosh^2[(g - \ln r)/2]$.

The found properties enable us to construct steady-state solutions for the semi-linear oscillator.

3 Threshold equation

3.1 Derivation procedure

As we know, detuning Ω changes to $-\Omega$ during the phase conjugation. On the other hand, the ordinary mirror, see Figure 1a, transforms wave 3 into wave 4 without any frequency change. Therefore, the only way to construct a steady-state frequency non-degenerate solution for the semi-linear oscillator is to accept that both $\pm\Omega$ components are present in each of the oscillating amplitudes. This means that two round trips in the cavity are necessary to return to the initial state.

We search thus for a steady-state solution in the form

$$\begin{aligned} A_{3,4}(z,t) &= A_{3,4}^+(z)\, e^{i\Omega t} + A_{3,4}^-(z)\, e^{-i\Omega t} \\ \nu(z,t) &= \nu^+(z)\, e^{i\Omega t} + \nu^-(z)\, e^{-i\Omega t}. \end{aligned} \tag{10}$$

According to the results of the previous section, we have $A_3^{+*}(0)/A_4^-(0) = \rho(\Omega)$ and $A_3^-(0)/A_4^{+*}(0) = \rho^*(-\Omega)$. The boundary condition $A_3(l,t) = 0$ is automatically fulfilled. Additionally, we have from equations (3) the boundary conditions $A_4^{\pm}(0) = \sqrt{R}\,\exp(i\phi_0)\, A_3^{\pm}(0)$ for the $\pm$ components. Expressing $A_4^{\pm}(0)$ by $A_3^{\pm}(0)$ and ρ and multiplying these relations to each other we arrive easily at the threshold equation in the form $\rho(\Omega)\,\rho^*(-\Omega)\,R = 1$. Using equations (8), (9), we represent the threshold equation in the following final explicit form:

$$\frac{\sqrt{rR}\,\left(1 - e^{\Gamma_0 l}\right)}{1 + r\, e^{\Gamma_0 l}} = \pm 1. \tag{11}$$

This equation admits an important generalization. By repeating the derivation procedure with the coupled-wave equations for the case of dominating reflection grating (they are present, e.g., in [2,3]) one can arrive at the same threshold equation (11) if the definition of the pump ratio $r = I_2^l/I_1^0$ is changed to $r = I_1^0/I_2^l$.

3.2 General properties

The threshold equation (11) is complex. It is equivalent to two real algebraic equations in Ω, g, r, and R. These enable one to calculate the detuning Ω and the coupling strength $g \equiv \gamma_0 l$ as functions of the pump ratio r and the reflectivity R. The solution for $\Omega(r,R)$ and $g(r,R)$ is not unique, see below, it consists of a sequence of non-intersecting branches.

The phase ϕ_0, which is determined by the distance to the feedback mirror, does not enter the threshold equation and does not influence the threshold conditions.

By taking the absolute values of the left- and right-hand sides of $\rho(\Omega)\,\rho^*(-\Omega)\,R = 1$ and using equations (8), (9), we obtain the relation $|\rho(\Omega)|^2\,R = 1$. It can be interpreted as an equation of balance between the intensity gain and losses during a round trip in the cavity. However, it cannot be used for optimization of Ω; the latter is not a free parameter because of the necessity to equate the arguments (phases) of the left- and right-hand sides of equation (11). With given r and R, there are no internal additional free parameters within our model (except for Ω) to ensure the phase matching.

3.3 Analysis of threshold equation

We consider first the frequency degenerate case $\Omega = 0$ where $\Gamma_0 l = -g$. Two solutions for the coupling

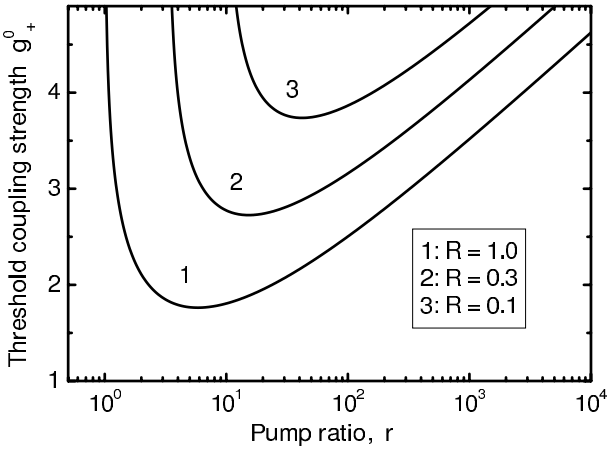

Fig. 2. Dependence $g^0_+(r)$ for three values of R.

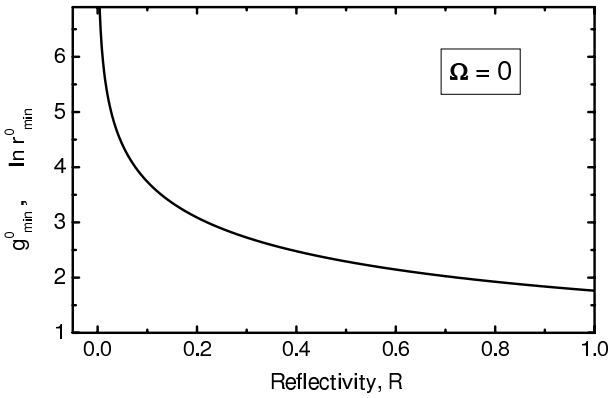

Fig. 3. Dependence of $g^0_{min} \equiv \ln(r^0_{min})$ on the reflectivity R.

strength g, that correspond to the signs $\pm$ in equation (11), are

$$g^0_\pm = \ln\left(\frac{\sqrt{rR} \pm r}{\sqrt{rR} \mp 1}\right). \qquad (12)$$

According to this relation we have $g^0_\pm(r, R) = -g^0_\mp(r^{-1}, R)$. In other words, for each positive value of $g^0(r)$ we have the opposite negative value $g^0(r^{-1})$. It is sufficient thus to consider the dependence $g(r, R) > 0$. One can check that it is given by $g^0_+(r, R)$.

Curves 1, 2, and 3 in Figure 2 show the dependence $g^0_+(r)$ for three representative values of the reflectivity R in a logarithmic scale for the pump ratio r. Each curve possesses a minimum. The position of the minimum r_{min} and the corresponding minimum value of the coupling strength $g^0_{min} = g^0_+(r_{min})$ depend on R. These dependences are given by the relations $r^0_{min}(R) = R^{-1}(2 + R + 2\sqrt{1+R})$ and $g^0_{min}(R) = \ln[r^0_{min}(R)]$. With the reflectivity R decreasing from 1 to 0, the values of r^0_{min} and g^0_{min} increase from $\simeq$5.8 and 1.76, respectively, to infinity, see Figure 3. The negative values of g^0, given by the branch g^0_-, can be obtained by the inversion of the curves presented in Figure 2 with respect to the point $g = 0$, $r = 1$.

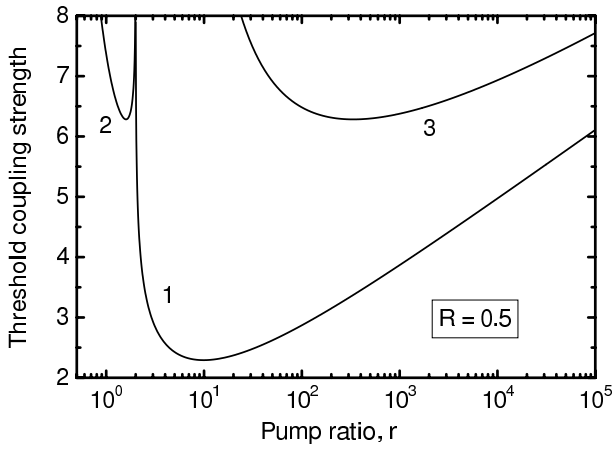

Fig. 4. Threshold value of g versus r for $R = 0.5$ and different branches: curves 1, 2, and 3 are plotted for branches g^0_+, g^1_+, and g^1_-, respectively.

The branches $g(r, R)$ and $\Omega(r, R)$ with $\Omega \neq 0$ obey the complex equation

$$\frac{g}{1 + \Omega^2 t_r^2}\left(1 + i\Omega t_r\right) = \ln\left(\frac{\sqrt{rR} \pm r}{\sqrt{rR} \mp 1}\right) \qquad (13)$$

that follows from equation (11). The logarithm in the right-hand side is understood according to the definition of the function of a complex variable Z, $\ln Z = \ln|Z| + i\arg(Z)$. The solutions with $\Omega \neq 0$ are possible only for $(\sqrt{rR} \pm r)/(\sqrt{rR} \mp 1) < 0$ when the argument of this expression is $\pi \pm 2\pi n$ with n being an integer.

The lowest branches for $g(r, R)$ and the corresponding branches for $\Omega(r, R)$ are given by

$$g^1_\pm = L_\pm + \frac{\pi^2}{L_\pm}\,; \qquad \Omega_\pm t_r = \frac{s\,\pi}{L_\pm}, \qquad (14)$$

where $L_\pm = \ln\left[-(\sqrt{rR} \pm r)/(\sqrt{rR} \mp 1)\right]$ and s acquires the values $+1$ and -1 independently of the $\pm$ signs. In other words, we have two opposite values of Ω for each allowed value of g. Furthermore, one can check that $g^1_\pm(r, R) = -g^1_\mp(r^{-1}, R)$, i.e., the dependence of g on $\log r$ is even and we can restrict again our analysis to the positive values of the coupling strength. As follows from equations (14), the minimum possible positive threshold value of g is 2π for both $\pm$ branches; it is attained for $L_\pm = \pi$ and $|\Omega|t_r = 1$.

Curves 2 and 3 in Figure 4 show the dependences $g^1_\pm(r)$ for $R = 0.5$; curve 1, shown for comparison, refers to the branch $g^0_+(r)$ with $\Omega = 0$. One sees that both $g^1_\pm$ branches allow positive values of the coupling strength. The branch g^1_+ exists within a narrow window of r; it is separated from the branch $g^0_+(r)$. The branch g^1_- exists within a relatively wide range of r; it co-exists with the g^0_+ branch. As follows from the data of Figure 4, only frequency non-degenerate oscillations are possible within the interval of pump ratio $1 \lesssim r \lesssim 2$ for sufficiently large values of the coupling strength. For larger values of r, degenerate and non-degenerate oscillations can compete with each other

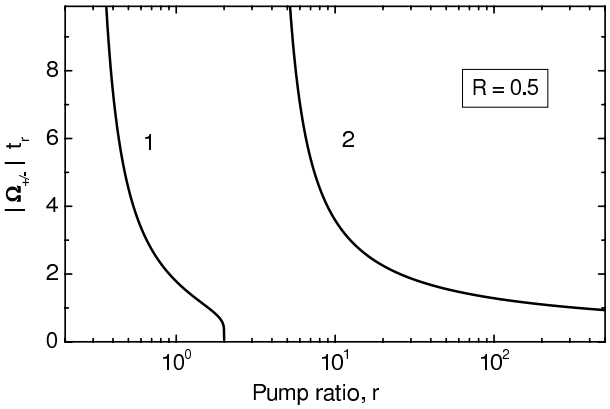

Fig. 5. Dependence $|\Omega_{\pm}(r)|$ for $R = 0.5$; lines 1 and 2, are plotted for the + and − branches, respectively.

for $g > 2\pi$. For the chosen value of the reflection coefficient R, the absolute minimum of the coupling strength, $g_{min} \simeq 2.3$, corresponds to a degenerate oscillation, $\Omega = 0$.

With decreasing R, the minima of curves 2 and 3 shift towards each other and the minimum of curve 1 shifts upwards and (simultaneously) to the right, see also Figure 3. For sufficiently small values of the reflection coefficient, $R < 7.5 \times 10^{-3}$, the minimum threshold value of the coupling strength corresponds to frequency non-degenerate oscillations (with $\Omega \neq 0$).

Figure 5 shows the dependences $|\Omega_{\pm}(r)|$ for $R = 0.5$. Note that Ω_+ turns to zero at $r \simeq 2$, which corresponds to the point separating curves 1 and 2 in Figure 4.

4 Temporal approach

It is not difficult to obtain exact results for the temporal evolution of the oscillation amplitudes within the undepleted pump approximation. They show explicitly that $A_{3,4}$ grow/decay exponentially in time above/below the threshold.

Let us search for the amplitudes in the form [compare with Eqs. (10)]

$$A_{3,4}(z,t) = [A^{+}_{3,4}(z)\, e^{i\Omega t} + A^{-}_{3,4}(z)\, e^{-i\Omega t}]\, e^{pt}$$
$$\nu(z,t) = [\nu^{+}(z)\, e^{i\Omega t} + \nu^{-}(z)\, e^{-i\Omega t}]\, e^{pt}\,, \quad (15)$$

where the increment p and the frequency detuning Ω are arbitrary real parameters. As earlier, equations (5) couple with each other the variables $A_3^{+*}, A_4^{-}, \nu^{-}$ and the variables $A_3^{-*}, A_4^{+}, \nu^{+}$. One can check that the solution for A_3^{+*}, A_4^{-} meeting the boundary condition $A_3^{+}(l) = 0$ is now

$$\begin{pmatrix} A_4^- \\ A_3^{+*} \end{pmatrix} = C_1 \left[\begin{pmatrix} A_1^0 \\ A_2^{l*} \end{pmatrix} e^{\Gamma z} + \begin{pmatrix} I_2^l/A_1^{0*} \\ -A_2^{l*} \end{pmatrix} e^{\Gamma l} \right], \quad (16)$$

where C_1 is an arbitrary complex constant and the rate of spatial changes Γ is

$$\Gamma = -\frac{\gamma_0}{1 + (p - i\Omega) t_r}. \quad (17)$$

This rate depends on the increment p; for $p = 0$ we have $\Gamma = \Gamma_0$. The amplitude ν^{-} can be readily expressed by A_4^{-}, A_3^{+*}.

Analogously we obtain for A_3^{-*}, A_4^{+} under the condition $A_3^{-}(l) = 0$:

$$\begin{pmatrix} A_4^+ \\ A_3^{-*} \end{pmatrix} = C_2 \left[\begin{pmatrix} A_1^0 \\ A_2^{l*} \end{pmatrix} e^{\Gamma^* z} + \begin{pmatrix} I_2^l/A_1^{0*} \\ -A_2^{l*} \end{pmatrix} e^{\Gamma^* l} \right], \quad (18)$$

where C_2 is a new arbitrary complex constant.

To describe the semi-linear oscillator, we have to satisfy additionally the boundary conditions $A_4^{\pm}(0) = \sqrt{R}\, e^{i\phi_0}\, A_3^{\pm}(0)$. Substituting $A_4^{\pm}(0)$ and $A_3^{\pm}(0)$ from equations (16) and (18), we obtain easily a set of linear uniform algebraic equations for C_1 and C_2^*. Equating to zero the determinant of this set (the solvability condition) and using equation (17), we arrive at the necessary dispersion equation for the increment p and the frequency detuning Ω:

$$\frac{g}{1 + p\, t_r - i\Omega t_r} = \ln\left(\frac{\sqrt{rR} \pm r}{\sqrt{rR} \mp 1} \right). \quad (19)$$

Its right-hand side is generally complex. For $p = 0$ we return to the threshold equation (13).

Consider now what follows from equation (19). In the region of r, R where the bracket in the right-hand side is positive (it corresponds to $\Omega = 0$) we have

$$p\, t_r = \frac{g}{g_{\pm}^0} - 1, \quad (20)$$

where $g_{\pm}^0(r,R)$ are the threshold values of the coupling strength for $g \gtrless 0$ from Section 3. Thus, the increment p is negative below threshold, tends to zero when approaching the threshold (which means the critical slowing down phenomenon [15]), and increases linearly with increasing supercriticality parameter $g - g_{\pm}^0$. The generation onset can indeed be interpreted as the instability of the state with $A_{3,4} = 0$.

Let now the bracket in equation (19) be negative, i.e., the imaginary part of the right-hand side be equal to $\pm\pi$ and $\Omega \neq 0$. In this case, we obtain:

$$p\, t_r = \frac{g}{g_{\pm}^1} - 1\,; \qquad |\Omega| = |\Omega_{\pm}|\, \frac{g}{g_{\pm}^1}, \quad (21)$$

where $g_{\pm}^1(r,R)$ and $|\Omega_{\pm}| = \pi/|L_{\pm}(r,R)|$ are the threshold values of g and $|\Omega|$ from Section 3. Again, we have the critical slowing down when the coupling strength g is passing its threshold value $g_{\pm}^1$. It is interesting that the frequency detuning becomes larger than its threshold value during an exponential growth of the oscillation amplitudes for $|g| > |g_{\pm}|$.

Note finally that the remark about validity of the threshold analysis for the case of dominating reflection grating, which is made in Section 3, is fully applicable to the temporal analysis of the oscillation instability. The above results are valid in the reflection case if we invert the definition of the pump ratio r.

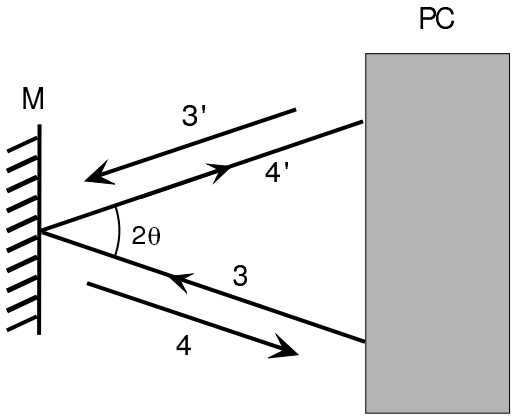

Fig. 6. Geometrical scheme for angularly split oscillation waves; M is ordinary mirror and PC is photorefractive crystal.

5 Angular split of oscillation waves

The above analysis admits one more important generalization. The oscillation waves can be incident not normally onto the feedback mirror within the experimental arrangement shown in Figure 1a. This possibility is illustrated by Figure 6. Wave 3 is incident onto the mirror M at a small angle θ to be reflected into wave $4'$. Wave $4'$, in turn, creates counter-propagating phase-conjugate wave $3'$. This wave, being reflected by the mirror, gives rise to wave 4 whose phase-conjugate counterpart is wave 3. Within this scheme we have not one but two spatial gratings with grating vectors $\mathbf{K} = \mathbf{k}_1 - \mathbf{k}_4 = \mathbf{k}_3 - \mathbf{k}_2$ and $\mathbf{K}' = \mathbf{k}_1 - \mathbf{k}'_4 = \mathbf{k}'_3 - \mathbf{k}_2$. The angle θ can be considered as an additional free parameter for minimization of the threshold coupling strength.

Within the undepleted pump approximation, the amplitudes $A'_{3,4}, \nu'$, which are relevant to the K' grating, obey the same set of equations as the amplitudes $A_{3,4}, \nu$ for the K grating, i.e., set (6). The difference between the coupling constants γ'_0 and γ_0 in these sets is negligible for $\theta \ll 1$. Waves $3'$ and 4 (as well as waves 3 and $4'$ are coupled only via the feedback mirror. As earlier, each of the wave amplitudes $A_{3,4}$, $A'_{3,4}$ consists of the $\pm$ components which are proportional to $\exp(\pm i\Omega t)$ and the amplitude ratio $\rho(\Omega)$, see equation (10), is the same for the pairs $3, 4$ and $3', 4'$.

With these preliminaries, a derivation of the threshold conditions is reduced to manipulation of a linear set of algebraic equations. It is not difficult to show that the generalized model possesses exactly the same threshold characteristics as the above considered basic model. The angular split θ does not lead to lowering oscillation threshold.

6 Summary

We have presented above a full-scale analysis of the threshold conditions for the semi-linear coherent photorefractive oscillator. This analysis is based on the conventional coupled-wave equations for the wave and grating amplitudes. It includes both the steady-state and temporal approaches and is free of any a priori assumptions about the amplitude and phase matching. The main outcomes of this analysis are:

- determination of the lowest branches for the threshold value of the coupling strength as function of the pump ratio and the feedback-mirror reflectivity;
- determination of the corresponding branches for the frequency detuning between the pump and oscillation waves;
- the absence of influence of a small angular split for the oscillation waves on the threshold behavior;
- identity of the behavior of the semi-linear oscillator in the cases of dominating transmission and reflection grating within the undepleted pump approximation.

Consider now the relationship between our analysis of the threshold behavior of the semi-linear oscillator and the previous steady-state analysis presented in [12–14]. The main assumption of these papers, expressed in our terms, is that the fulfillment of an energy balance equation for a round trip in the cavity, $|\rho(\Omega, g, r)|^2 R = 1$, is sufficient for the oscillation. Within this assumption, the detuning Ω was considered as a free parameter for minimization of the coupling strength $g(\Omega, r, R)$. It was found in this manner that the minimum value of g does not correspond to $\Omega = 0$ in a certain range of r, R.

The present analysis has shown that the threshold equation (11) is real (and equivalent to the above balance equation) only for $\Omega = 0$. In the general case ($\Omega \neq 0$), the threshold equation is complex, which means that the condition of phase matching after a round trip in the cavity can be fulfilled only for special values of Ω. In other words, the frequency detuning cannot be considered as a free parameter for minimization of the coupling strength. Taking into account other possible varying parameters of the model (the distance to the feedback mirror and the angular split for the oscillation waves) does influence the threshold behavior and cannot lead to an automatic fulfillment of the condition of phase matching. It is useful to mention also that the present analysis shows the presence of two minima in the threshold diagram for non-degenerate oscillations (Fig. 4) as opposed to the single minimum expected in references [12–14].

The most interesting feature of the *experiments* [12,13] with the semi-linear oscillator is the appearance of frequency splitting between the oscillation and pump waves with changing pump ratio r. Within our model, such a split is possible only for sufficiently high values of the coupling strength, $|g| > 2\pi$. This value is higher than the values that were estimated in the experiments of [12,13]. However, since the value of g was not determined independently in the above experiments, it is not excluded that the observations are compatible with the basic model.

The general points of agreement between experiment and the heuristic analysis [12–14], such as the linear intensity dependence of the frequency splits and the presence of a window of the pump ratio where the non-degenerate regime takes place, are compatible with our analysis.

Additional experiments are needed to establish precise values for the coupling strength in relation with the thresholds for non-degenerate oscillation, in view of the present theoretical results.

We remark finally that the present model employs some simplifying assumptions like the plane wave approximation or the absence of transverse structure. Inclusion of these effects can modify the threshold values of the coupling strength and frequency detuning.

Financial support from Université de Bourgogne is gratefully acknowledged.

References

1. M. Cronin-Golomb, B. Fisher, J.O. White, A. Yariv, IEEE J. Quant. Electron. **QE-20**, 12 (1984)
2. S. Kwong, M. Cronin-Golomb, A. Yariv, IEEE J. Quant. Electron. **QE-20**, 1508 (1986)
3. *Photorefractive Materials and Their Applications, I*, edited by P. Günter, J.-P. Huignard, Vol. 62 of Topics in Applied Physics (Springer-Verlag, Berlin, 1989)
4. S. Odoulov, M. Soskin, A. Khyzhnyak, *Optical Coherent Oscillators with Degenerate Four-Wave Mixing* (Harwood Academic Publishers, Chur, London, 1991)
5. L. Solymar, D.J. Webb, A. Grunnet-Jepsen, *The Physics and Applications of Photorefractive Materials* (Oxford, Clarendon Press, 1996)
6. J. Feinberg, R. Hellwarth, Opt. Lett. **5**, 519 (1980)
7. F.T. Arecchi, G. Giacomelli, P.L. Ramazza, S. Residori, Phys. Rev. Lett. **65**, 2531 (1990)
8. S.R. Liu, G. Indebetouw, J. Opt. Soc. Am. B **9**, 1507 (1992)
9. K. Staliunas, M.F.H. Tarroja, G. Slekys, C.O. Weiss, L. Dambly, Phys. Rev. A **51**, 4140 (1995)
10. C. Denz, M. Schwab, M. Sedlatschek, T. Tschudi, T. Honda, J. Opt. Soc. Am. B **15**, 2057 (1998)
11. P. Mathey, Appl. Phys. B **80**, 463 (2005)
12. P. Mathey, S. Odoulov, D. Rytz, Phys. Rev. Lett. **89**, 053901 (2002)
13. P. Mathey, S. Odoulov, D. Rytz, J. Opt. Soc. Am. B **19**, 2967 (2002)
14. M. Grapinet, P. Mathey, S. Odoulov, D. Rytz, Appl. Phys. B **79**, 345 (2004)
15. H. Haaken, *Synergetics* (Springer-Verlag, Berlin, 1978)